Available online at www.sciencedirect.com
SCIENCE DIRECT®
Journal of Nuclear Materials 353 (2006) 19–26
journal of nuclear materials
www.elsevier.com/locate/jnucmat

First-principle study of B1-like thorium carbide, nitride and oxide

I.R. Shein, K.I. Shein, A.L. Ivanovskii *

Institute of Solid State Chemistry, Ural Branch of the Russian Academy of Sciences, Pervomaiskaya Str. 91, Ekaterinburg 620219, Russia

Received 11 November 2005; accepted 1 February 2006

Abstract

The electronic properties of cubic (B1-type) thorium carbide (ThC), nitride (ThN) and meta-stable monoxide (ThO) were calculated systematically using the full-potential linearized augmented plane wave method with the generalized gradient approximation for the exchange and correlation potential (LAPW–GGA). The structural parameters, bulk modulii, electronic bands, densities of states (DOS), charge distributions were obtained and compared with available experimental data and other calculations. The theoretical spectra of non-metal *K*-edge X-ray emission (XES) and absorption (XAS) of these materials are presented and discussed.

1. Introduction

The binary compounds formed by thorium with light elements such as C, N, and O have attracted interest because of their high density, good thermal conductivity and some other interesting properties as alternative fertile materials to be used in nuclear breeder systems etc., see [1–4]. Among them thorium monocarbide (ThC) and mononitride (ThN), which crystallize in the rock salt (B1-like) structure are known, where carbon or nitrogen atoms occupy the octahedral interstitial sites in the face-centered cubic thorium sublattice. On the contrary, B1-like thorium monoxide (ThO, thorium valence state +2) is thermodynamically unstable, and its decomposition $ThO \rightarrow Th\ (metal) + ThO_2$ occurs [5].

As a result, for fluorite-like thoria the Th^{+4} valence states and the tetrahedral coordination of oxygen atoms are stabilized. Note that the occurrence of the B1 structure type for the thorium oxide and the preference of the octahedral (six-fold) in comparison with tetrahedral (four-fold) oxygen coordination can be achieved by means of a partial substitution of oxygen by carbon (or by nitrogen) resulting in the formation of the thermodynamically stable oxicarbide (oxinitride) phases [6].

The physical properties and chemical behavior exhibited by the metal carbides, nitrides and oxides are closely related to the electronic structure and chemical bonding, depending on the competition of metal–metal/metal–non-metal interactions and the contributions of metallic, covalent, and ionic bonding to the cohesive energy [7]. However,

* Corresponding author. Tel.: +7 343 3755331; fax: +7 343 3744495.
E-mail address: ivanovskii@ihim.uran.ru (A.L. Ivanovskii).

0022-3115/$ - see front matter © 2006 Elsevier B.V. All rights reserved.
doi:10.1016/j.jnucmat.2006.02.075

contrary to other B1-like MX compounds (where M = 3d–5d or 4f and 5f metals), the reliable results for the electronic properties and bonding mechanism for the corresponding thorium phases are lacking so far.

Several earlier experimental and theoretical studies of the electronic structure of these materials have been performed, the results (obtained before 1994) are reviewed in Refs. [2,3,7]. New interesting data were received during the last period, especially concerning Th nitride. Quite recently, the FLAPW calculations of the enthalpies of formation of ThN in comparison with others actinide nitrides AnN were reported [8]. The electronic properties of ThN films are examined by photoelectron spectroscopy [9]. Molecular dynamics simulations were performed to evaluate some thermo-physical properties for ThN [10]; the equation of state and bulk modulus for ThN are treated in the framework of an ionic model [11]. The tight-binding LMTO method was employed recently, in order to evaluate the densities of states (DOS) and charge distribution patterns of Ti, V, Zr, Hf compared with U and Th monocarbides [12]. Concerning the thorium oxides, only stable fluorite-like ThO_2 was investigated. In particular, the elastic properties were calculated [13,14]; the $O_{4,5}$ X-ray emission spectra of the thorium dioxide, reflecting the occupied Th 6p and 5f states are obtained [15], as well as the core level binding energies for ThO_2 are measured by XPS [16].

In this paper, we concentrate on the effects of non-metal sublattice (X = C, N and O) on the electronic properties of B1-like thorium compounds and present the results of first-principle investigations of cubic ThC, ThN phases, as well as isostructural metastable ThO. The optimized structural parameters, bulk modulii, electronic bands, DOS and charge distributions were calculated. Moreover, for all ThX phases we have also calculated for the first time the theoretical shape of X-ray emission (XES) and absorption (XAS) non-metal Kα spectra. As is known, these are powerful tools to probe the filled and empty electronic states of materials and possess the advantage to measure the bulk electronic structure in contrast to photoelectron spectroscopy [9], do not demand the preparation of atomically clean and ordered surface, that is difficult for ThX phases usually prepared as polycrystalline samples [1–3]. Thus, the theoretical analysis of the XES and XAS spectra can be useful for a discussion of applicability of these methods for the characterization of various thorium compounds with light elements.

2. Method of calculations

The band-structure calculations of the all mentioned B1 thorium compounds were done by means of the full potential all-electron DFT method with mixed basis APW + lo (LAPW) method implemented in the WIEN2k suite of programs [17]. The generalized gradient correction (GGA) to exchange-correlation potential of Perdew, Burke, and Ernzerhof [18] was used. The sphere radii were chosen as 2.8 for Th and 1.55 a.u. for C, N and O. The plane-wave cutoff K_{cut} is determined by $R_{mt}K_{cut}$ =9.0. Blöchl's modified tetrahedron method [19] was employed for the DOS calculations. The carbon, nitrogen and oxygen Kα XES, XAS spectra ($2p \leftrightarrow 1s$ transitions) were calculated using Fermi's golden rule and the matrix elements between the core and valence states (following the formalism of Neckel et al., Ref. [20]); as implemented in the WIEN2k code. The calculated spectra include broadening for the spectrometer and core and valence lifetimes.

3. Results and discussion

3.1. Structural and elastic properties

The calculated equilibrium lattice constants, bulk moduli and its pressure derivative for thorium compounds, derived from the fit to Murnaghan's equation of state are given in Table 1. First of all, our results for the equilibrium lattice constants a_0 for thorium carbide and nitride are in a good accordance with the experimental data, and the deviation between the experimental and theoretical value does not exceed about 1.0% for ThC and 0.6% for ThN. The better agreement with the experiment for ThN is due to the strong stoichiometry of thorium nitride, while in the measured thorium carbide samples the variable amount of C-vacancies is present [3].

Oppositely, the calculated equilibrium lattice constant ($a_0 = 5.111$ Å) for metastable ThO is far from the experimental value ($a_0 = 5.320$ Å, i.e. the deviation is higher than 4%) derived from X-ray diffraction studies [6] for annealed samples, which contain the admixtures of ThO_2 ($a_0 = 5.597$ Å) and metallic α-Th ($a_0 = 5.084$ Å). Thus, the full occupancy of the octahedral interstitial sites in thorium by carbon or nitrogen atoms leads to Th–Th distance expansion at about 0.215 Å (5.98%) and 0.069 Å (1.90%) for ThC and ThN, respectively.

Table 1
Calculated lattice constants a_0 (Å), bulk modulii B_0 (GPa) and their energy derivatives B′ for ThC, ThN and metastable ThO in comparison with available experimental data

Phase (parameter)	ThC		ThN		ThO
	Our data	Experiment	Our data	Experiment	
a_0	5.3879	5.335–5.344 [3]	5.1813	5.156–5.152 [2]	5.1114
B_0	131.89	109 [22]; 125 [2]	179.63	175 [21]	177.73
B′	2.73	3.1 [22]	4.15	4.0 [21]	7.57

For ThO the distance between the nearest Th atoms are almost equal to those in α-Th: their difference is less 0.005 Å, i.e. about 0.5%.

Next, we have examined the bulk modules B_0 for ThX. The calculated B_0 for ThC (about 132 GPa) is much larger than B_0 of metallic α-Th (about 60–62 GPa [23]), i.e. a pronounced increase of structural rigidity from metal to carbide due to the direct Th–C bonding formation occurs, as well as for other B1-like metal monocarbides, see [24]. The experimentally estimated ThC bulk modulus B_0 falls in the wide range from 73.9 GPa (the result of extrapolation to stoichiometric $ThC_{1.0}$ from the elastic constants c_{ij}, obtained for the $ThC_{0.063}$ single crystal [25]) to 107 [22] and 125 GPa (cited in [2]). Thus, in relation to the two last values, our calculations reproduce the experiment with accuracy at about 23–6%. In our opinion this may be an effect of the sub-stoichiometry of the ThC samples as mentioned above. Note, that the simplified ASA-LMTO calculations of B_0 (about 43 GPa [12]) underestimate the ThC bulk modulus value more than twice.

A much better agreement of the calculated B_0 with the experimental data has been achieved for ThN (the deviation is less than 2.5%, Table 1) because of a very limited homogeneity region of the mononitride phase. Concerning the metastable ThO, to the best of the authors knowledge, there are no published experimental data on the bulk modulus of this material.

In general, the presence of carbon or nitrogen in metal compounds leads to the hybridized M–(C,N) bonding, and their strengthening (accompanied by the M–M bonding) determines lattice constants and bulk modulii. It is known for the actinide B1-like compounds that small cell volumes lead to higher bulk modulii [1]. Accordingly, our results show that thorium nitride has higher B_0 than Th carbide. This trend (as observed also for other metal carbides and nitrides [24,26,27]) is supported by experiment, and can be interpreted as a result of the enhancement of Th–N (as compared with Th–C) bonding because nitrogen has one more valence electron than carbon, so that the metal–non-metal bonding strength in nitride is higher than that in carbide. Additionally, the increase of the metal bands filling leads to some enhancement of the metal–metal bonding. Finally, our calculations predict that B_0 for ThO is only about six percent smaller than for thoria (186.91 GPa) which has been calculated by us in the same approach. The experimental value for the bulk modulus of ThO_2 is found to be (195 ± 2) GPa [14].

3.2. Electronic structure

Fig. 1 illustrates the band dispersion curves along some high symmetry directions in the Brillouin zone of all studied B1-like ThX phases, the main band structure parameters are given in Table 2. Obviously, that the real band structure of these materials is determined by at least several factors: geometrical (cell volume), electronic (electron concentration per cell) and chemical (electronegativities of atoms). Nevertheless the band structure pictures and band ordering for the all ThX phases are very similar. Namely in the region at about −17 to −18 eV below the Fermi level (E_F) ThX spectra are characterized by the low-energy semi-core Th 6p bands; in Fig. 1, these curves are not shown. The next energetically low-lying bands are derived from the X 2s states which do not contribute to the interatomic bonding. The energies of these bands decrease rapidly as going from ThC to ThO, and in the latter case the oxygen 2s states are placed below the Th 6p states. Note, that these bands display a maximum dispersion between Γ and L points of values 2.82, 2.80 and 1.95 eV for ThC, ThN and ThO, respectively. This difference depends on the competition of the energy separation between X 2s and the nearest X 2p and Th 6p bands. These gaps (Δ(X 2p − X 2s)/Δ(X 2s − Th 6p) are 2.90/6.05 (ThC), 5.80/2.20 (ThN) and 12.55/1.05 eV (ThO).

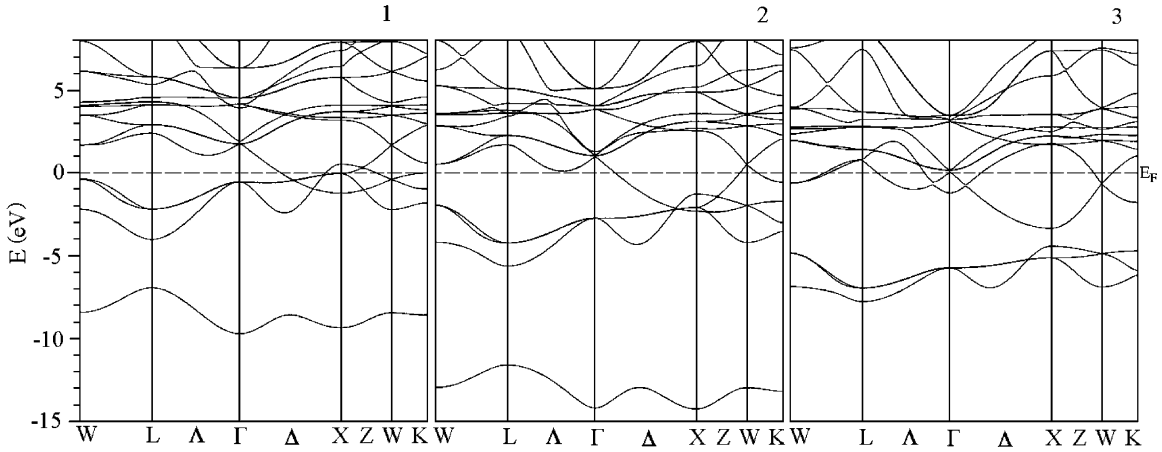

Fig. 1. Electronic band structures of B1-like ThC (1), ThN (2) and metastable ThO (3). The Fermi level $E_F = 0$ eV.

Table 2
Band structure parameters (in eV), total densities of states at the Fermi level N(E_F), (in states/eV cell) and specific heat coefficient γ (in mJ mol^{-1} K^{-2}) obtained from FLAPW–GGA for ThC, ThN and metastable ThO

Phase (parameter)	ThC	ThN	ThO
Width of the X 2s band	2.82	2.80	1.95
Gap between X 2s and X 2p bands	2.90	5.85	12.55
Width of the occupied X 2p + Th d,f bands	4.15	5.80	7.75
Width of the occupied Th d,f bands	1.30	2.10	3.45
Width of the occupied X 2p bands	4.15	3.40	3.22
Gap between X 2p and Th d,f bands	–	–	1.08
N(E_F)	0.749	1.158	0.564
γ	1.867	2.737	1.333

The next three bands originate mainly from X 2p states. For ThC these bands are partially filled and cross the E_F around X. Going from ThC to ThO the number of valence electrons increase from eight to ten, and the Fermi level moves up in energy. In result, for ThN and ThO the X 2p bands are fully occupied. In the vicinity of the Fermi level the thorium 6d-like bands are placed, whereas the Th 5f bands are at about 4–5 eV higher.

As can be seen from Fig. 1, there are an overlap and a mixing between Th and X 2p bands below E_F; this is indicative for the covalent metal–non-metal interactions for these compounds. In ThN and ThO, more valence electrons presented in the unit cell, which leads to additional occupation of thorium bands near E_F. The Fermi level crosses the thorium bands which contribute to the DOS at the Fermi level (N_F), i.e. all ThX materials are metallic-like. The possibility of ThX magnetization was examined; for this purpose the spin-polarized calculations, assuming initial ferromagnetic state for ThX phases, were carried out. It was found that the ground state for all materials is non-magnetic, without any localized atomic magnetic moments. This result is in accordance with observed paramagnetism of ThC and ThN [2,3].

In Fig. 2, we show the total and site-projected density of states for ThX. For ThC the DOS of the valence and conduction bands are separated by a pseudo gap. The valence band ranging from −4.15 eV to E_F is of mixed Th (6d + 5f)–C 2p character. In turn, Th 6d (e_g) states forming strong covalent Th–C σ-like bonds, are located below 6d (t_{2g}) states, which are responsible for π-like Th–C, as well as Th–Th bonding.

In order to illustrate the interatomic bonds in B1-like ThX materials, we display as example the charge distribution map in ThC (100) plane, as well as the charge density profiles along Th–C and Th–Th bonding lines as function of interatomic distances d, Fig. 3. We find the near-spherically distribution of electron density around thorium and carbon atoms, with rather small density value between them. This is typically for crystals with the NaCl structure having the ionic bonding due to the charge transfer from the metals to the non-metal atoms. However, the bonding in ThC cannot be described as a exclusively ionic type. Really, the charge density profiles along Th–C and Th–Th bonding lines demonstrates the overlap of the corresponding electronic states, which constitute the covalent (Th–C) as well as the metallic-like (Th–Th) parts of the bonding. Thus, our calculations show the simultaneous existence in the thorium monocarbide (as well as in the

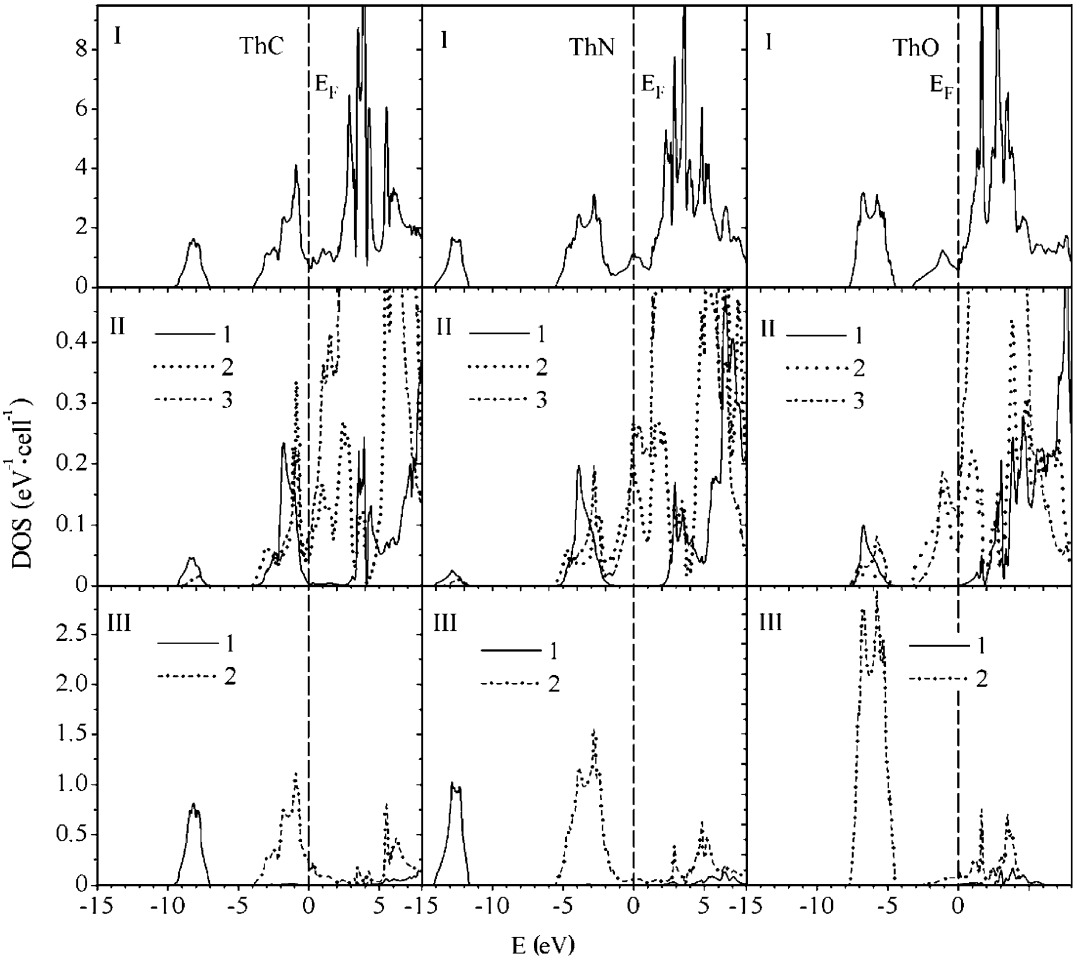

Fig. 2. Total (I) and partial (II, III) densities of states (DOS) of B1-like ThC, ThN and metastable ThO. Partial DOS of Th states (panel II): 1 – Th 6d (e_g), 2 – Th 6d (t_{2g}), 3 – Th 5f; and non-metal states (panel III): 1 – X 2s and 2 – X 2p; where X = C, N or O, are presented. Vertical lines – Fermi energy.

other cubic ThX phases) of ionic, covalent and metallic components of bonding.

Note that the comparable contributions in the near-Fermi region of ThC provide also the Th 5f states. As a result, the near-Fermi states are formed exclusively by Th 6d (t_{2g}), 5f and carbon C 2p states. Moreover, as can be seen from Table 3, the large contribution in N(E_F) follows from C 2p states. This unusual situation differs dramatically from the others 3d–5d or 5f metal carbides, for which the near-Fermi region formed mainly of 3d–5d or 5f states, respectively [1,7]. For ThN and ThO the near-Fermi states are also composed by comparable contributions of Th 6d and 5f states, whereas the contributions of (N,O) 2p states become much smaller. For the row of thorium phases (ThC → ThN → ThO, i.e. by adding one electron per cell), N(E_F) changes non-monotonically: grows at about 0.41 (ThC → ThN) and decreases at 0.59 states/eV cell (ThN → ThO); in the latter case E_F is located in a local DOS minimum between Th 6d (t_{2g}) and 5f states. These results showing that the density of conduction states of ThN is higher compared with ThC coincide in general with the experimental data based on the measurement of specific heat coefficient γ [2,3]. However, our results are in contradiction to experiment [25] about the further growth of the density of conduction states, going from ThN to stable B1-like thorium monosulfide, with the same electronic concentration (10 electrons per cell) as ThO. This demonstrates clearly the difference of the electronic structure for isostructural and isoelectonic ThS and ThO.

The above calculations allow us to obtain the specific heat coefficient γ for ThX materials, assuming

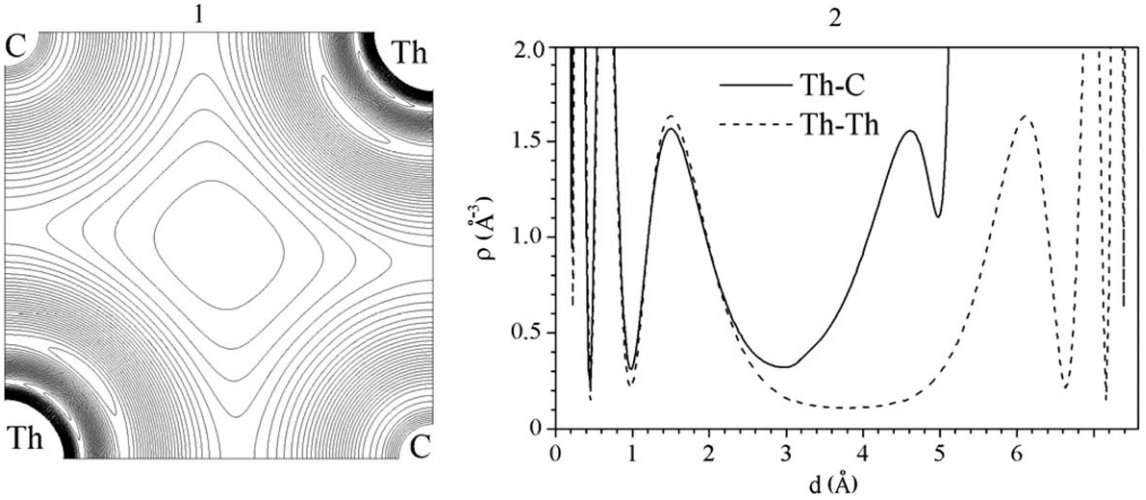

Fig. 3. Charge density map in the (1 0 0) plane of B1-like thorium monocarbide (1) and the charge density profiles along Th–C and Th–Th bonding lines (2).

Table 3
Site-projected *l*-decomposed DOSs at the Fermi level $N^l(E_F)$ (in states/eV) for ThC, ThN and metastable ThO according to FLMTO–GGA calculations

Phase	Th 6d	Th 5f	(C,N,O) 2p
ThC	0.051	0.083	0.209
ThN	0.202	0.264	0.066
ThO	0.055	0.112	0.048

the free electron model, $\gamma = (\pi^2/3)N(E_F)k_B^2$, Ref. [28], see Table 2. The calculated γ for ideal ThC is about 1.87 mJ mol^{-1} K^{-2}, and is a bit less, than calorimetrically obtained γ ranging from 2.12 to 2.90 mJ mol^{-1} K^{-2} for various ThC_x samples, for which the carbon deficiency leads to increase of the γ values [1]. The earlier full-relativistic APW calculation without lattice relaxation gives for ThC the value of $\gamma = 2.6$ mJ mol^{-1} K^{-2}. For ThN our estimation of $\gamma = 2.74$ mJ mol^{-1} K^{-2} is comparable with experiment (3.12 mJ mol^{-1} K^{-2} [2]). For ThO, γ is smallest among the considered ThX materials, Table 2.

3.3. X-ray emission and absorption spectra

As is known, the intensity (I) of the X-ray emission (XES) and absorption spectra (XAS) in the dipole approximation is determined by the DOS and the matrix element and can be written as

$$I(E,e) \sim E^3\Sigma \mid \langle \mathrm{f} \mid e \cdot r \mid \mathrm{i} \rangle|^2 \delta(E_F + E - E_i),$$

where $\langle$f| and |i$\rangle$ refer to the final and initial one-electron states, E_i and E_F are the corresponding energy eigenvalues of the states involved in the transition. The same expression may be also used for the calculation of the XAS shapes provided the intensity on the left hand side is replaced by the linear absorption coefficient. In our case, Kα (2p $\rightarrow$ 1s transition) XES probes directly the distributions of occupied carbon, nitrogen or oxygen 2p DOS, whereas AES spectra reflect their unoccupied 2p states.

Fig. 4 shows the emission and absorption (C,N,O) *K*-edge spectra in B1-like ThX materials obtained from our FLAPW calculation; all the spectra are depicted by aligning the Fermi level. For XES lines, as going from ThC to ThO, the main peaks (A, B, C) are shifted downwards and are located at -1.05 (ThC), -2.85 (ThN) and -5.80 eV (ThO); besides, additional sub-peaks a′, a″ (ThC) and b′ (ThN) are clearly shown. The assignment of these peaks can be done considering the DOS of the ground state (Fig. 2). For example for ThN, the XES peaks b′ and B arise from N 2p states hybridized with Th 6d states of mainly e_g symmetry and mixed Th $\{6d(t_{2g}) + 5f\}$ states, respectively. Thus, the maxima energy distances A–a′ (0.75 eV) and B–b′ (1.1 eV) reflect the growth of Th $6d(e_g)$–$6d(t_{2g})$ band splitting in ThN as compared with ThC. On the contrary, a symmetrical O*K* XES spectral shape for ThO is obtained, where oxygen 2p bands are separated from thorium bands by a gap.

Much more complicated are the XAS shapes of ThX phases. For example, the carbon *K*-edge absorption spectrum of ThX includes, besides the near-Fermi peak A′ and the most intensively

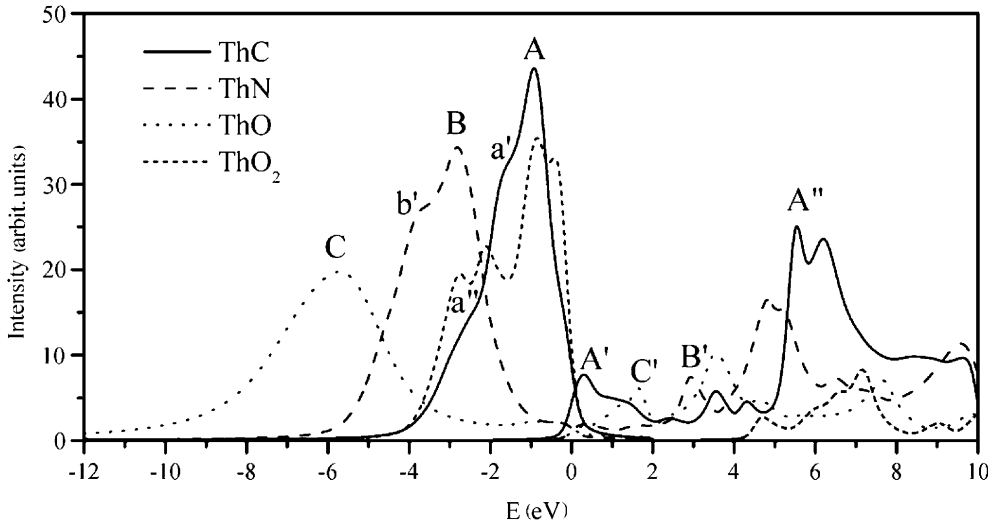

Fig. 4. Theoretical shapes of (C,N,O) *K*-edge X-ray emission (XES) and absorption (XAS) spectra of B1-like ThC, ThN and metastable ThO in comparison with fluorite-like thoria.

double-shaped peak (A″, in the region at about 5.7–6.2 eV), also a set of clearly resolved peaks, reflecting the contributions of anti-bonding carbon 2p-like states into empty thorium bands. Contrary to ThC, the lowest XAS peaks C′ and B′ for ThO and ThN are located at 1.7 and 2.9 eV, respectively, showing very small amounts of (N,O) 2p states near the Fermi energy.

Finally, our calculations show that the XES and XAS shapes (including the number of spectral peaks, their relative intensity and their energy positions in a spectrum) for B1-like monoxide ThO and fluorite-like dioxide ThO_2 change drastically, see Fig. 4. Thus, these results show that X-ray emission and absorption spectroscopy near the (C,N,O) *K*-edge may be very useful techniques for detailed probe of the bulk-electronic structure of ThX phases. They also provide a wide prospect for studying the possible oxygen positions (six-fold versus four-fold) in more complicated Th-based materials – for example, for various solid solutions such as thorium oxicarbides or oxicarbonitrides.

4. Conclusions

In this paper by means of first principle calculations we have performed a systematic study of structural parameters, bulk modulii, electronic bands, densities of states, charge distributions as well as the shapes of non-metal *K*-edge X-ray emission and absorption spectra of B1-like thorium monocarbide, mononitride and metastable monoxide, which are discussed in comparison with available experimental data and other calculations. The important conclusions of our calculations are the following.

The calculated equilibrium lattice constants a_0, bulk modulii B_0 and specific heat coefficients γ are in good agreement with experiment for perfectly stoichiometric ThN, whereas for ThC the discrepancy is larger. This may be an effect of the sub-stoichiometry of the ThC samples. The values of a_0, B_0 and γ for metastable ThO are predicted for the first time.

We note that the bonding behavior in the ThX phases is a combination of covalent, ionic and metallic characters. Comparable contributions of Th 6d (predominantly of t_{2g} symmetry) and 5f states are responsible for the formation of Th–Th and Th–X bonds. This situation differs considerably from the related B1-like 3d–5d or 5f metal-based phases, for which the interatomic bonds are formed mainly with participation of 3d–5d or 5f metal states.

We have calculated for the first time the (C,N,O) *K*-XES and XAS shape in ThC, ThN, ThO and fluorite-like ThO_2 and found that these spectra are highly sensitive to the chemical nature of non-metal lattice, and also to positions of the light elements. Thus, our results show that these techniques may be very useful for the detailed probe of the bulk-electronic structure, as well as for study of coordination states of light elements in thorium-based materials such as oxicarbides and oxicarbonitrides, or solid solutions ThC–ThC_2; note, that

thorium dicarbide contains strongly coupled C–C pairs as structural elements. The analysis of the competition of various interstitial lattice sites filled by non-metal atoms (or by their pairs), depending on the variable concentration of lattice vacancies is a subject of our forthcoming study.

References

[1] A.J. Freeman, G.H. Lander (Eds.), Handbook of the Physics and Chemistry of the Actinides, North-Holland, Amsterdam, 1985.
[2] R. Benz, A. Naoumidis, Thorium, Compounds with Nitrogen, Gmelin Handbook of Inorganic Chemistry, eighth ed. Thorium supplement, vol. C3, Springer, Berlin, 1987.
[3] H. Kleykamp, Thorium Carbides. Gmelin Handbook of Inorganic and Organometallic Chemistry, eighth ed. Thorium supplement, vol. C6, Springer, Berlin, 1992.
[4] A.H.M. Evensen, R. Catherall, P. Drumm, P. Van Duppen, O.C. Jonsson, E. Kugler, J. Lettry, O. Tengblad, V. Tikhonov, H.L. Ravn, Nuclear Inst. Method. Phys. Res. B 126 (1997) 160.
[5] U. Benedict, J. Less-Common Met. 128 (1987) 7.
[6] R.J. Ackermann, E.G. Rauh, J. Inorg. Nucl. Chem. 35 (1973) 3787.
[7] V.A. Gubanov, A.L. Ivanovskii, V.P. Zhukov, Electronic Structure of Refractory Carbides and Nitrides, Cambridge, University Press, 1994 (2005, second ed.).
[8] D. Sedmidubsky, R.J.M. Konings, P. Novak, J. Nucl. Mater. 344 (2005) 40.
[9] T. Gouder, L. Havela, L. Black, F. Wastin, J. Rebizant, P. Boulet, D. Bouexiere, S. Heathman, M. Idiri, J. Alloys Comp. 336 (2002) 73.
[10] J. Adachi, K. Kurosaki, M. Uno, S. Yamanaka, J. Alloys Comp. 394 (2005) 312.
[11] M. Aynyas, S.P. Sanyal, P.K. Jha, Phys. Stat. Sol. B 229 (2002) 1459.
[12] T. Das, S. Deb, A. Mookerjee, Physica B 367 (2005) 6.
[13] S. Li, R. Ahuja, B. Johansson, High Pressure Res. 22 (2002) 471.
[14] J.S. Olsen, L. Gerward, V. Kanchana, G. Vaitheeswaran, J. Alloys Comp. 381 (2004) 37.
[15] Yu.A. Teterin, V.A. Terekhov, A.Yu. Teterin, K.E. Ivanov, I.O. Utkin, A.M. Lebedev, L. Vukchevich, J. Electr. Spectr. Related Phenom. 96 (1998) 229.
[16] S. Anthonysamy, G. Panneerselvam, S. Bera, S.V. Narasimhan, P.R. Vasudeva Rao, J. Nucl. Mater. 281 (2000) 15.
[17] P. Blaha, K. Schwarz, G.K.H. Madsen, D. Kvasnicka, J. Luitz, in: K. Schwarz (Ed.), WIEN2K, An Augmented Plane Wave Plus Local Orbitals Program for Calculating Crystal Properties, Techn. Universität Wien, Austria, 2001.
[18] J.P. Perdew, S. Burke, M. Ernzerhof, Phys. Rev. Lett. 77 (1996) 3865.
[19] P.E. Blöchl, O. Jepsen, O.K. Andersen, Phys. Rev. B 49 (1994) 16223.
[20] A. Neckel, K. Schwarz, R. Eibler, P. Rastl, Microchim. Acta Suppl. 6 (1975) 257.
[21] L. Gerward, J.S. Olsen, U. Benedict, J.P. Itié, J.C. Spirlet, J. Appl. Cryst. 18 (1985) 339.
[22] L. Gerward, J.S. Olsen, U. Benedict, J.P. Itié, J.C. Spirlet, J. Appl. Cryst. 19 (1986) 308.
[23] K. Hachiy, Y. Ito, Physica B 262 (1999) 233.
[24] G.V. Samsonov, I.M. Vinizkii, Refractory Compounds, Moskwa, Nauka, 1976 (in Russian).
[25] J.D. Greiner, D.T. Peterson, J.F. Smith, J. Appl. Phys. 48 (1977) 3357.
[26] J.C. Grossman, A. Mizel, M. Cote, M.L. Cohen, S.G. Louie, Phys. Rev. B 60 (1999) 6343.
[27] Z. Wu, X.-J. Chen, V.V. Struzhkin, R.E. Cohen, Phys. Rev. B 71 (2005) 214103.
[28] C. Kittel, Introduction to Solid State Physics, fourth ed., Wiley, New York – London – Sydney – Toronto, 1986.